Dopant Induced Room Temperature Ferromagnetism in Spintronic SnO_2: Co Nanoparticles

E. Pradyumna, N. Sreelekha, D. Amaranatha Reddy, K.R. Gunasekhar, K. Subramanyam

Abstract — Pristine and Co doped SnO_2 nanoparticles were synthesized in aqueous solution by facile chemical co-precipitation method with polyethylene glycol (PEG) as a capping agent. The as prepared samples were characterized by X-ray diffraction (XRD), transmission electron microscopy (TEM), high resolution transmission electron microscopy (HRTEM), Fourier transform infrared (FTIR) spectra and vibrating sample magnetometer (VSM). XRD patterns revealed that particles of all samples were crystallized in single phase rutile type tetragonal crystal structure ($P4_2/mnm$) of SnO_2. TEM images indicated spherical shape of nanoparticles with a size ranging from 25-35 nm. FTIR spectra suggested that the PEG simply coexisted with the SnO_2 surface nanoparticles and inhibited the agglomeration of the nanoparticles. Magnetization measurements revealed that all the Co doped SnO_2 nanoparticles exhibited ferromagnetic signal which became stronger with increasing Co content. Variation of ferromagnetic order with Co content from vibration sample magnetometer is endorsed to the anti-ferromagnetic (AFM) interactions among the magnetic ions as anticipated by the bound magnetic polarons (BMP) theory.

Keywords— Chemical synthesis, PEG, TEM, BMP model,

I. Introduction

Conventional electronics utilizes only the charge degree of freedom of the carrier. Recently, a new field named Spintronics has emerged wherein it is envisioned that novel functional devices can be fabricated if the charge as well as the spin degrees of freedom can be combined which have improved efficiency and less power consumption. So, oxide based diluted magnetic semiconductors have been the focus of widespread research in the last decade, due to the growing interest in finding materials for the emerging technology of Spintronics. The fascinating incidence of room temperature ferromagnetism (RTFM) in naturally non-magnetic oxides under certain conditions have also attracted much attention in the field of condensed matter physics and there is major consensus that point defects play a fundamental role in the emergence of this phenomenon [1-4]. The root of the observed ferromagnetism has been somewhat controversial in some systems, particularly when the materials were made-up using deposition techniques in reducing atmospheres because of the possible isolation of transition metal particles. Nevertheless, to produce the origin of ferromagnetism from the predictable diluted magnetic state, it is very important to investigate FM in doped and undoped semiconducting oxide powders because only powders can reflect intrinsic magnetic properties of material [5-6]. Of all the oxide based semiconductors, SnO_2 is a technologically resourceful and significant non toxic n-type semiconducting material for many applications especially in nanocrystalline form such as gas sensors, optoelectronic devices, dye based solar cells, liquid crystal display transistors and secondary lithium batteries owing to its wide band gap (3.6 eV at 300 K), relatively large excitation binding energy and good optical transparency in the visible region [7-12]. However, studies on the effect of Co doping on the properties of SnO_2 are sparingly available [13-15] even the available reports mainly focused on either bulk materials or thin films. A. Bouaine et al. [13] reported structural, optical, and magnetic properties of Co-doped SnO_2 powders synthesized by the co-precipitation technique and they found mixture of paramagnetic and anti-ferromagnetic behavior for Co-doped SnO_2 with no sign of ferromagnetism. Ogale et al. [16] found a giant magnetic moment of 7.5+0.5μB/Co with high T_C (650 K) in Co-doped SnO_2 thin films fabricated by pulsed laser deposited (PLD). Punnoose et al. [17] also observed RTFM in 1% Co doping, however it is decreased completely for higher Co doping. Further, the development of future optoelectronics and other devices requires new materials in reduced dimensionality and size, such as nanoparticles.

We have reported a systematic study on the structural, optical and magnetic properties of Cr doped SnO_2 nanoparticles and observed well defined RTFM hysteresis loop for 1% Cr concentration [18]. Recently we have also reported the effect of Co co-doping, Mn co-doping and Cu co-doping on the structural, optical and magnetic properties of SnO_2:Cr DMS nanoparticles [19-21]. In the present work a systematic investigation was carried out on the effect of Co doping on the morphological, structural and magnetic properties of SnO_2: Co nanoparticles. In this study $Sn_{1-x}Co_xO_2$ (x = 0.00, 0.01, 0.03, 0.05 and 0.07) nanoparticles were prepared by chemical co-precipitation method and the effect of Co doping on the morphological, structural, magnetic properties is reported.

II. Experimental

$Sn_{1-x}Co_xO_2$ (x= 0.00, 0.01, 0.03, 0.05 and 0.07) nanoparticles capped with PEG were synthesized by simple co-precipitation method. All chemicals $SnCl_4.5H_2O$, $CoCl_2.6H_2O$, NH_4OH and PEG-400 used in the present study are of AR grade and used without further purification. Aqueous solutions of precursors (0.2 M)

Revised Version Manuscript Received on October 17, 2015

E. Pradyumna, Department of Mechanical Engineering, Amrita School of Engineering, Coimbatore, Tamil Nadu- 641112, India.

N. Sreelekha, Department of Physics, Raghu Engineering College, Visakhapatnam, Andrapradesh-531162, India.

D. Amaranatha Reddy, Department of Chemistry and Chemical Institute for Functional Materials, Pusan National University, Busan, 609735, Republic of Korea.

K.R. Gunasekhar, Department of Instrumentation and Applied Physics, Indian Institute of Science, Bangalore - 560012, India.

K. Subramanyam, Department of Physics, Raghu Engineering College, Visakhapatnam, Andrapradesh-531162, India.

Published By:
Blue Eyes Intelligence Engineering
& Sciences Publication Pvt. Ltd.

were separately prepared as per stoichiometric ratio and stirred for 30 min. In this solution NH_4OH (28%) solution was added drop wise in very controlled manner to maintain the chemical homogeneity. The addition of NH_4OH was stopped when pH of the solution reached to 9 at room temperature and added 2 ml of surfactant (PEG-400) under vigorous stirring for 8 hr. The precipitate was filtered out separately and washed with de-ionized water to remove unnecessary impurities formed during the synthesis process. The obtained product was placed in oven for 14 hr at 60^o C and the dried samples were grounded for half an hour and then annealed at 600^o C for 3 hr to obtain $Sn_{1-x}Co_xO_2$ nanoparticles.

The samples of $Sn_{1-x}Co_xO_2$ (x= 0.00, 0.01, 0.03, 0.05 and 0.07) were subjected to various characterization studies. Chemical analysis was carried out using scanning electron microscopy (SEM) with EDAX attachment (CARL-ZEISS EVO MA 15). Structural investigations were done by ''Seifert 3003 TT X-ray Diffractometer'' with Cu-Kα radiation with a wavelength of 1.542 Å. Crystal structure and crystallite size were obtained from XRD data. The particle size and structure confirmations were done by Phillips TECHNAI FE 12, Transmission Electron Microscope (TEM). FTIR studies were carried out using Thermo Nicolet FTIR-200 thermo Electron Corporation and the thermal analysis was done by TG/DTA using EXSTAR 6000 series thermal analyzer. Room temperature magnetization was recorded using a Lakeshore vibrating sample magnetometer, VSM 7410.

III. Results and Discussion

3.1 Elemental analysis

Elemental analysis was carried out in permutation with the result obtained from SEM using EDX technique. The EDX measurements were performed randomly at several spots across the samples to show that there is no microphase separation or compositional inhomogeneous at a sub micrometer level. Fig. 1 shows the EDX spectrum shows $Sn_{1-x}Co_xO_2$ (x=0.01) nanoparticles, besides the lines of the constitutive elements Sn, O and Co, the EDX spectrum gives no indication for other elements, confirming the phase-purity of the sample.

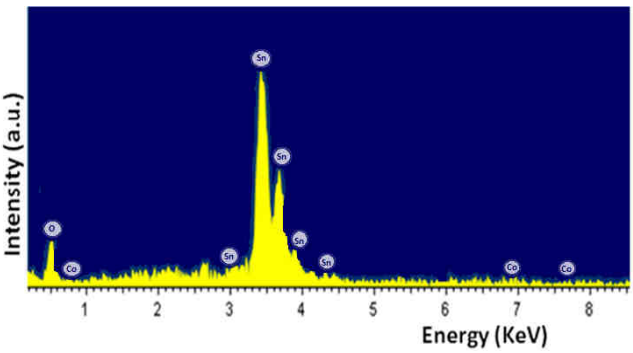

Fig. 1 EDAX spectra of $Sn_{1-x}Co_xO_2$ (x= 0.01) nanoparticles.

3.2. Morphological studies

Fig. 2(a–d) displays SEM images of the pure and Co doped SnO_2 nanoparticles respectively. SEM micrographs manifest the microstructure with fine particles on the surface of the powders. As seen in these images, that the agglomeration is decreasing with doping. It is evident from the images that the morphologies of Co-doped samples are dissimilar from that of the undoped samples. In undoped samples only clouds of agglomerations are seen where as in doped samples the agglomerated particles are conspicuously visualized. It is also noticed that in doped samples, the agglomerated particles appear to be nearly spherical with the distribution becoming nearly homogeneous.

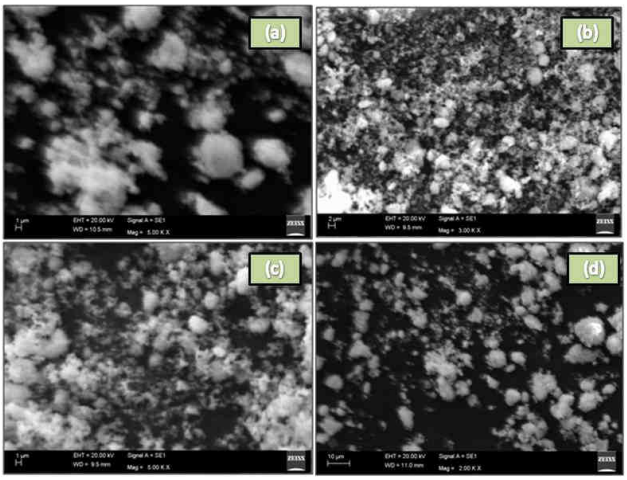

Fig. 2 (a-d) SEM images of $Sn_{1-x}Co_xO_2$ (x= 0.00, 0.01, 0.03 and 0.05) nanoparticles

3.3 Structural analysis

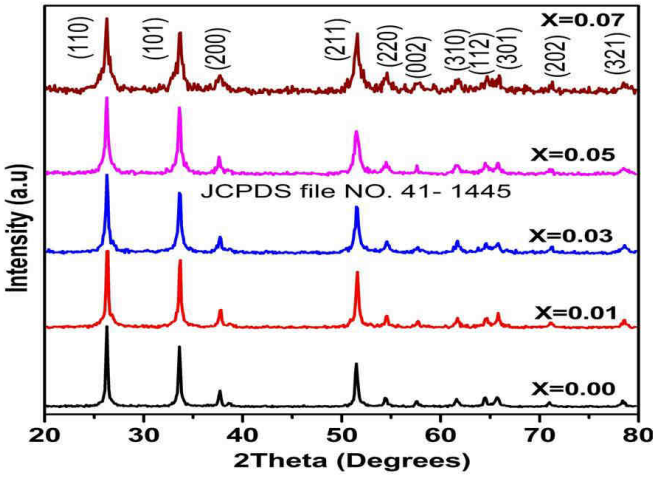

Fig. 3 XRD patterns of $Sn_{1-x}Co_xO_2$ (x= 0.00, 0.01, 0.03, 0.05 and 0.07) nanoparticles.

The XRD patterns of the synthesized pure and Co doped SnO_2 nanoparticles are displayed in Fig. 3. The sharp diffraction peaks provide evidence that the as prepared nanoparticles have high crystallinity. The XRD patterns of the doped and undoped nanoparticles show a single phase with rutile type tetragonal crystal strucure as per the standard card (JCPDS No. 41-1445). No peaks corresponding to other phases or impurities could be seen within the resolution limit. The broadening of XRD peaks are indicative of the nanosize of the particles. Further, the peak positions shift towards higher 2θ values with increasing Co concentration. This clearly implies lattice compression consistent with the smaller ionic radius of Co^{2+} (0.058 nm) compared to that of Sn^{4+} (0.069 nm), confirming the incorporation of the dopant as substituent in the synthesized SnO_2 nanoparticles. The average nanocrystallite size (D), was estimated from the full width at half maximum (FWHM) of the most prominent

Published By:
Blue Eyes Intelligence Engineering
& Sciences Publication Pvt. Ltd.

XRD (110) broadening peak using the Debye-Scherer formula, $D=0.89\lambda/\beta\cos\theta$, where λ is the wavelength of X-ray radiation, β is the full width at half maximum of the peak at diffraction angle θ [22] and the average crystallite sizes were found to be decreased with increasing the doping concentration is in the range of 28-35 nm. The XRD spectra have also been used to study the crystallanity of the samples. The doping of the Co in SnO_2 not only reduces the particle size but also degrades the crystallanity of the nanoparticles. As the Co doping concentration increases the intensity of the XRD peak decreases and FWHM increases, which is due to the degradation of the crystallanity. This means that even though Co ions occupy the regular site of Sn^{4+}, it produces crystal defects around the dopants and the charge imbalance arising from this defect changes the stoichiometry of the samples. A. Bouaine et al. [13] and Shendong Zhuang et al. [14] also observed similar decrease of particle size with increasing the dopant concentrations.

3.4 TEM and HRTEM analyses

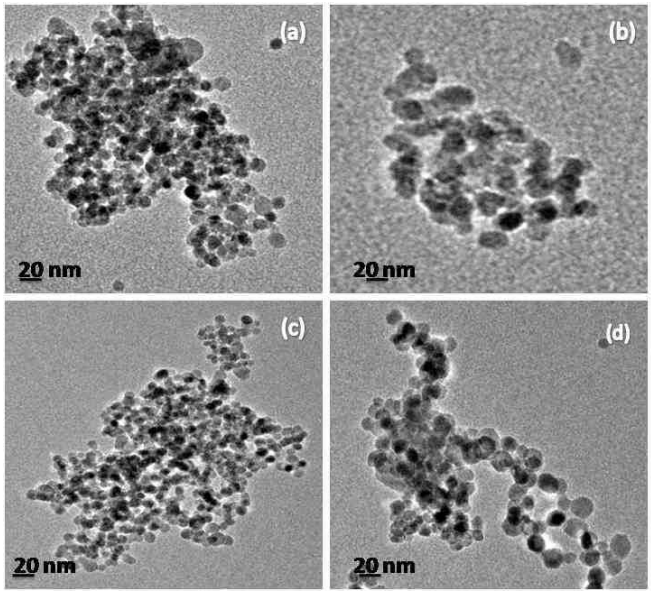

Fig. 4 (a-d) TEM images of $Sn_{1-x}Co_xO_2$ (x= 0.00, 0.01, 0.03 and 0.05) nanoparticles.

Fig. 4 (a-d) shows typical TEM images of $Sn_{1-x}Co_xO_2$ (x= 0.00, 0.01, 0.03 and 0.05) nanoparticles. It was clear from the TEM micrographs that the morphology of the particles are found to be nearly spherical in shape and it is also evident that the uniform distribution of particles by the addition of PEG to the host matrix. The average size of nanoparticles obtained from TEM analysis is in the range of 25-35 nm. Fig. 5 (a-b) shows the HRTEM images of pure and Co doped SnO_2 nanoparticles respectively.

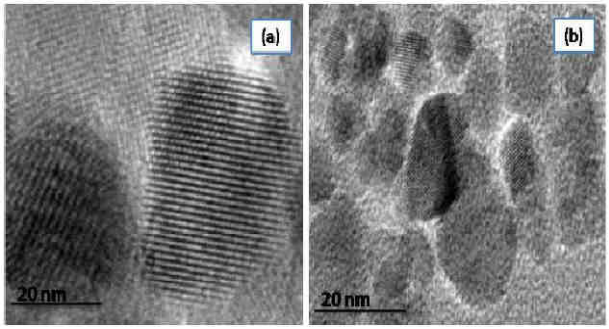

Fig. 5 (a-b) HRTEM images of the $Sn_{1-x}Co_xO_2$ (x= 0.00, and 0.01) nanoparticles.

3.5 FTIR analysis

FTIR spectra of $Sn_{1-x}Co_xO_2$ (x = 0.00, 0.01, 0.03, 0.05 and 0.07) nanoparticles, capped with PEG recorded at room temperature in the wavelength range of 4000–400 cm^{-1} are shown in Fig. 6. The peaks at 3472 cm^{-1}, 1638 cm^{-1}, 1562 cm^{-1}, 1404 cm^{-1} and 624 cm^{-1} are found in the spectra of the present synthesized samples. The broad band around 3472 cm^{-1} is assigned to the O-H stretching vibration because all FTIR spectra are recorded by mixing samples with KBr. Hence there may be some adsorbed water vapor, as KBr is hygroscopic. As there are no other functional groups from aliphatic chains falls those are in the region from 2000 to 1300 cm^{-1}, peaks at 1638 and 1562 cm^{-1} can also be attributed to O–H group. The absorption peaks appeared at 1573 cm^{-1} and 1404 cm^{-1} is endorsed to the symmetric C-H stretching vibrations of the PEG molecules [23, 24]. Finally broad peak at 624 cm^{-1} in undoped and Co-doped SnO_2 samples in the infrared spectra is owing to the stretching vibrations of O-Sn-O it confirms the bonding of metal-oxygen as present in SnO_2 [25]. The absence of extra peaks related to CoO modes at 664 cm^{-1} and 588 cm^{-1} in the infrared spectra indicated that Co is completely miscible in SnO_2. This analysis could provide evidence that surface of the SnO_2: Co nanoparticles were capped by PEG with inclusion of Co ions. Thus, FTIR results confirm that the nanoparticles formed are of SnO_2.

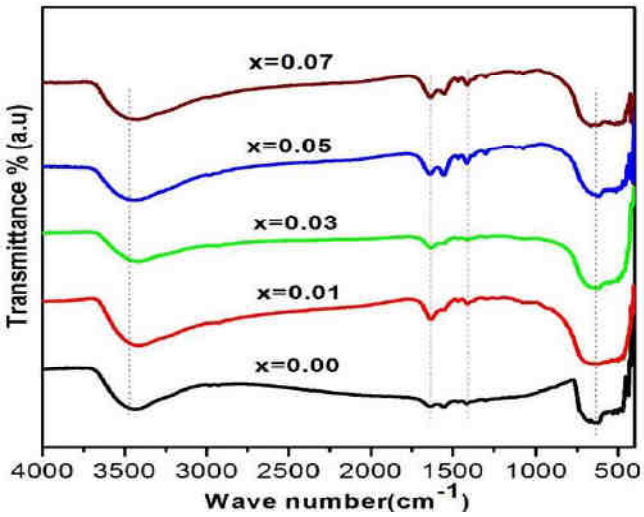

Fig. 6 FTIR spectra of $Sn_{1-x}Co_xO_2$ (x= 0.00, 0.01, 0.03, 0.05 and 0.07) nanoparticles.

3.6 Thermal analysis

In order to examine the thermal stability of the calcined precursor of $Sn_{1-x}Co_xO_2$ nanoparticles, its weight loss was monitored by heating the material at the rate of 10°C per minute in the presence of nitrogen atmosphere. Fig. 7 shows the TGA plots for $Sn_{1-x}Co_xO_2$ nanoparticles in the temperature range 18-800°C. The first weight loss up to 152°C is due to the removal of absorbed water molecules and the second one in between 150 °C to 390 °C should be attributed to the decomposition of a part of polyethylene glycol [24]. Above the 390 °C decomposition of residual PEG leads to a further weight loss. After being heated to 800 °C the residue is SnO_2 which is the weight of the original sample.

Published By:
Blue Eyes Intelligence Engineering
& Sciences Publication Pvt. Ltd.

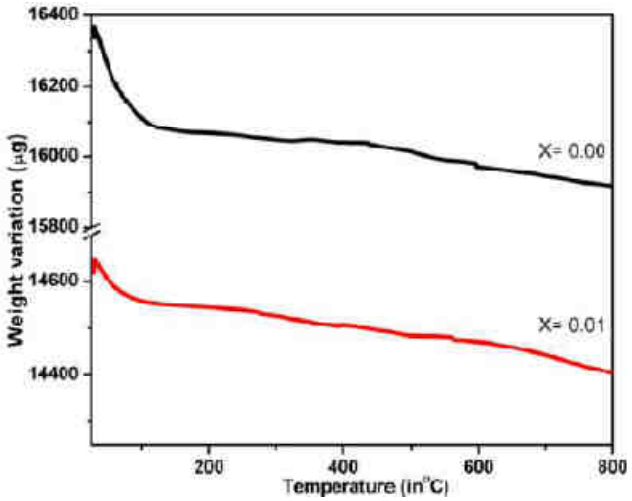

Fig. 7 TGA analysis of $Sn_{1-x}Co_xO_2$ (x= 0.00 and 0.01) nanoparticles.

3.7 Magnetic studies

Fig. 8 (a, b) shows the field-dependent magnetization (M–H) curves of $Sn_{1-x}Co_xO_2$ (x = 0.00, 0.01, 0.03, 0.05 and 0.07) nanoparticles, at room temperature in the field range of 0 to ±15000 Gauss. A distinctive diamagnetic behavior has been observed in the host SnO_2 and is attributed to the absence of unpaired electrons of its 'd' orbital. From the Fig. 8 (b) it is clear that Co doped SnO_2 nanoparticles shows hysteresis loop room temperature indicating that the samples exhibit ferromagnetic nature. Maximum saturation magnetization (M_S), 22.25 × 10^{-3} emu/g, for the 3 at.% Co doped SnO_2 nanoparticles and weak ferromagnetism of 7 at.% Co doped SnO_2 samples were observed in SnO_2 lattice. Magnetic parameters such as saturation magnetization (M_S), retentivity (M_R) and coercivity (H_C) obtained from the hysteresis loops are presented in Table. 1. The increasing spontaneous magnetic moment observed with increasing Co content indicates that only a fraction of Co ions is magnetically ordered with respect to the applied field. The origin of ferromagnetism in DMS is highly controversial and has been a subject of debate. The observed ferromagnetism of the present samples may be attributed to the secondary phases of cobalt oxides and Co clusters which were not detected within the detection limit of XRD instrumentation and in infrared spectra.

Hence the observed ferromagnetism could not be attributed to cobalt oxide. Even though number of mechanisms might be responsible, an effort has been made to explain this phenomenon using bound magnetic polarons (BMPs) model [26-27]. According to this model, the localized spins of the dopant ions interact with the charge carriers which are bound to a small number of defects such as oxygen vacancies, resulting in a magnetic polarization of the surrounding local moments. In the samples of present investigation, due to the substitution of Co ions for Sn site, number of free charge carriers and oxygen vacancies might have been introduced to maintain the charge neutrality leading to the formation of BMPs, which are coupled with the available small quantity of randomly distributed neighboring Co might be responsible for the observed magnetic states in the present synthesized samples. It is reported that the amount of Co ions and the separation between magnetic ions is indeed a crucial factor that decides magnetic response of the sample. Besides, according to the BMP model as the doping concentration increases anti-ferromagnetic interactions between neighboring Co-Co ions enhances and suppress the ferromagnetism in SnO_2: Co, which is observed in our present investigations. Shendong Zhuang et al. [14] also observed similar magnetic behavior with inclusion of Co in SnO_2 host matrix.

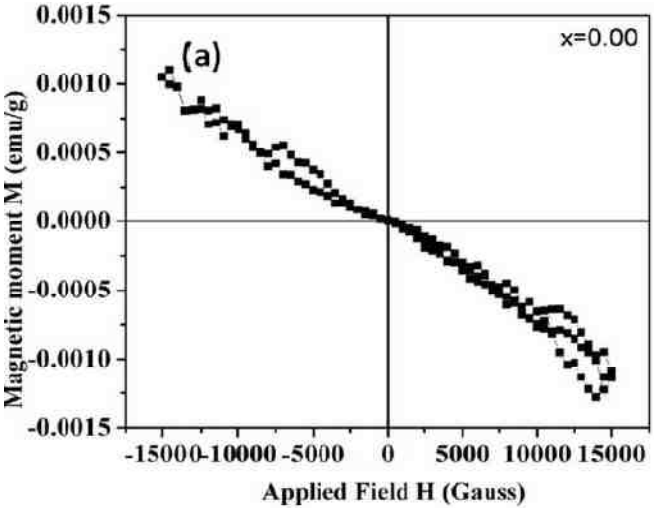

Fig. 8 (a) Room temperature M-H plots of $Sn_{1-x}Co_xO_2$ (x= 0.00) nanoparticles.

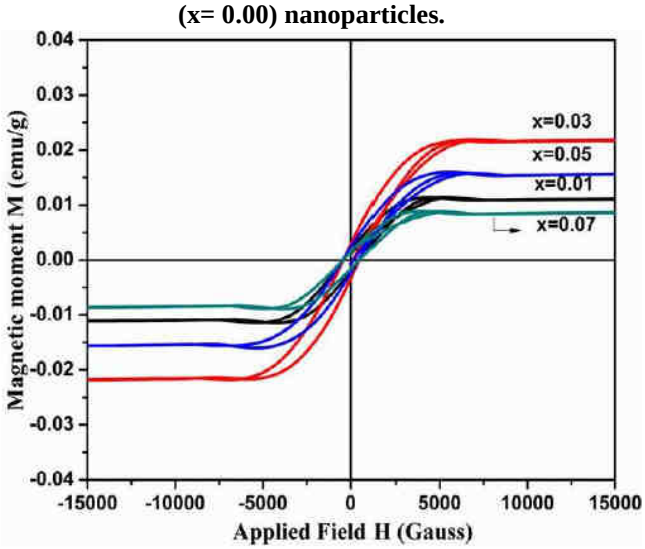

Fig. 8 (b) Room temperature M-H plots of $Sn_{1-x}Co_xO_2$ (x= 0.01, 0.03, 0.05 and 0.07) nanoparticles.

IV. Conclusions

In summary, pure and Co doped SnO_2 nanoparticles were successfully synthesized by the chemical co-precipitation method using PEG as the capping agent. Structural characterizations of the samples using XRD and FTIR patterns revealed that the SnO_2 crystallites with tetragonal rutile type structure formed under the synthesized temperature 600°C. TEM and HRTEM images show that the obtained particles were spherical and well dispersed with narrow size distribution. The BMP model is a reasonable explanation for observed room temperature ferromagnetism. Magnetic moment per Co^{2+} ion is increases at lower doping concentration whereas at higher doping concentration magnetic moment is decreases due to anti-ferromagnetic interactions takes place among the neighbor in Co^{2+} ions in the samples. The present investigations in our work suggests that Co doped SnO_2 may be potential DMS candidate for spintronic devices.

Published By:
Blue Eyes Intelligence Engineering
& Sciences Publication Pvt. Ltd.

Table. 1 Magnetic parameters $Sn_{1-x}Co_xO_2$ nanoparticles

Parameter ↓ / Sample →	x=0.01	x=0.03	x=0.05	x=0.07
Ms (emu/g)	11.13×10^{-3}	22.25×10^{-3}	15.71×10^{-3}	0.832×10^{-3}
M_R (emu/g)	1.03×10^{-3}	2.38×10^{-3}	2.21×10^{-3}	0.963×10^{-3}
Hc (Gauss)	408	447	435	396

Acknowledgments

The authors are thankful to Mr. N. Sivarama krishnan and Mr. Muttu kumar, SAIF, IIT Madras, Chennai for providing the VSM facility.

REFERENCES

1. H. Ohno, Making Nonmagnetic Semiconductors Ferromagnetic, Science 281 (1998) 951-956.
2. S.A. Wolf, D.D. Awschalom, R.A. Buhrman, J.M. Daughton, S. Von Molnar, M.L. Roukes, A.Y. Chtchelkanova, D.M. Treger, Spintronics: A Spin-Based Electronics vision for the Future, Science 294 (2001) 1488-1495.
3. G.A. Prinz, Magnetoelectronics, Science 282 (1998) 1660-1663.
4. J. K. Furdyna, Diluted magnetic semiconductors, J. Appl. Phys. 64 (1988) R29-64.
5. S. Datta, B. Das, Electronic analog of the electro-optic modulator, Appl. Phys. Lett. 56 (1990) 665–667.
6. C.B. Fitzgerald, M. Venkatesan, A.P. Douvalis, S Huber, J.M.D. Coey, T. Bakas, SnO_2 doped with Mn, Fe or Co: Room temperature dilute magnetic semiconductors, J. Appl. Phys 95 (2004) 7390–7392.
7. W. Zeng, T. Liu, D. Liu, E. Han, Hydrogen sensing and mechanism of M-doped SnO_2 (M=Cr^{3+}, Cu^{2+} and Pd^{2+}) nanocomposite, Sens. Actuators. B 160 (2011) 455–462.
8. D.S. Kumar, P.R. Carbarrocas, J.M. Siefert, in situ invistigations of the optoelectronic properties of transparent conducting oxide/ amorphous silicon interfaces, Appl. Phys. Lett. 54 (1989) 2088–2090.
9. S. Ferrere, A. Zaban, B.A. Gregg, dye sensitization of nanocrystalline tin oxide by perylene derivative, J. Phys. Chem. B 101 (1997) 4490–4493.
10. Y. Tachibana, K. Hara, S. Takano, K. Sayama, H. Arkawa, Investigations on anodic photocurrent loss processes in dye sensitized solar cells: comparison between nanocrystalline SnO_2 and TiO_2 films, Chem. Phys. Lett. 364 (2002) 297–302.
11. D. Wang, S. Wen, J. Chen, S. Zhang, F. Li, Microstructure of SnO_2, Phys. Rev. B 49 (1994) 14282–14285.
12. A.S.Yu, R. Frech, Coating of multi-wall carbon nanotube with SnO_2 films of controlled thickness and its applications for Li-ion battery, J. Power Sources. 104 (2002) 97-102.
13. A. Bouaine, N. Brihi, G. Schmerber, C. Ulhaq-Bouillet, S. Colis, A. Dinia, Structural, optical, and magnetic properties of Co-doped SnO_2 powders synthesized by the co-precipitation technique, J. Phys. Chem. C 111 (2007) 2924-2928.
14. Shendong Zhuang, XiaoyongXu n, YaruPang, HeLi,BinYu, Jingguo Hu, Variation of structural, optical and magnetic properties with Co-doping in $Sn_{1-x}CoxO_2$ nanoparticles, J. Magn. Magn. Mater., 327 (2013) 24–27.
15. Sunita Mohanty, S. Ravi, Ferromagnetism in Mechanically Milled $Sn_{1-x}Co_xO_2$ (x = 0 to 0.10) Compounds, J Supercond Nov Magn, 25 (2012) 1017–1023.
16. S.B.Ogale,R.J.Choudhary,J.P.Buban,S.E.Lofland,S.R.Shinde,S.N.Kale , V.N.Kulkarni, J.Higgins, C.Lanci, J.R.Simpson, N.D.Browning, S.D.Sarma, H.D. Drew, R.L.Greene, T.Venkatesan, High temperature ferromagnetism with a gaint magnetic moment in transparent Co doped SnO_2, Phy. Rev. Lett, 91(2003) 077205-211.
17. A. Punnoose, J. Hays, V.Gopal, V.Shutthanandan, Room temperature ferromagnetism in chemically synthesized $Sn_{1-x}Co_xO_2$ powders, Appl. Phys. Lett. 85 (2004) 1559.
18. K. Subramanyam, N. Sreelekha, G. Murali, D. Amaranatha Reddy, R.P. Vijayalakshmi, Structural, optical and magnetic properties of Cr doped SnO_2 nanopaerticles stabilized with poly ethylene glycol, Physica B, 454 (2014) 86–92.
19. K. Subramanyam, N. Sreelekha, G. Murali, D. Amaranatha Reddy, B. Poorna prakash, S. Ramu, R.P. Vijayalakshmi, Structural, optical and magnetic properties of chromium and manganese co-doped SnO_2 nanoparticles, Solid State Sciences, 39 (2015) 74-81.
20. K. Subramanyam, N. Sreelekha, G. Murali, D. Amaranatha Reddy, R.P. Vijayalakshmi, Enhanced room temperature ferromagnetism in polyethylene glycol capped $Sn_{0.99-x}Cu_xCr_{0.01}O_2$ nanoparticles, IJITEE, 4 (2014) 27–32.
21. K. Subramanyam, N. Sreelekha, G. Murali, D. Amaranatha Reddy, R.P. Vijayalakshmi, Influence of Co co-doping on structural, optical and magnetic properties of SnO_2:Cr nanoparticles, Superlattices Microstruct. 82 (2015) 207–218.
22. B.D. Cullity, Elements of X-Ray Diffraction, Wesley, London, 1978.
23. M. Sudha, S. Senthilkumar, R. Hariharan, A. Suganthi, M. Rajarajan, Synthesis, characterization and study of photocatalytic activity of surface modified ZnO nanoparticles by PEG capping, J. Sol-Gel Sci. Technol. 65 (2013) 301–310.
24. R. Hariharan, S. Senthil kumar, A. Suganthi, M. Rajarajan, Synthesis and characterization of doxorubicin modified ZnO/PEG nanomaterials and its photodynamic action, J. Photochem. Photobiol. B 116 (2012) 56-65.
25. S. Gnanam, V. Rajendran, Preparation of Cd-doped SnO_2 nanoparticles by sol–gel route and their optical properties, J Sol-Gel Sci Technol.56 (2010) 128–133.
26. A. Kaminski and S. Das Sarma, Polaron percolation in diluted magnetic semiconductors, Phys. Rev. Lett. 88 (2002) 247202-4.
27. J. M. D. Coey, M. Venkatesan and C. B. Fitzgerald, Donor impurity band exchange in dilute ferromagnetic oxides, Nat. Mater. 4 (2005) 173-179.

Published By:
Blue Eyes Intelligence Engineering
& Sciences Publication Pvt. Ltd.